Journal of Advanced Biomedical and Pharmaceutical Sciences

Journal Homepage: http://jabps.journals.ekb.eg

Headspace GC-MS and LC-MS based metabolomic study of Waterpipe smoke of unflavored and peach-flavored Moâssel with an insight into their health hazards

Ashraf N. E. Hamed[1*], Marwa M. Ismail[1], Usama R. Abdelmohsen[1,2], Amr A. Kamel[3], Mahmoud El-Daly[3], Mostafa A. Fouad[1], Amira R. Khattab[4], Mohamed S. Kamel[1,2]

[1]Department of Pharmacognosy, Faculty of Pharmacy, Minia University, 61519 Minia, Egypt.
[2]Department of Pharmacognosy, Faculty of Pharmacy, Deraya University, 61111 New Minia, Egypt.
[3]Department of Pharmacology and Toxicology, Faculty of Pharmacy, Minia University, 61519 Minia, Egypt.
[4]Department of Pharmacognosy, College of Pharmacy, Arab Academy for Science, Technology and Maritime Transport, Alexandria 1029, Egypt.

Received: November 20, 2020; revised: December 28, 2020; accepted: December 31, 2020.

Abstract

The wide prevalence of Waterpipe smoking in today's society has provoked us to study both chemical matrix and toxicological impact of two locally-produced Moâssel products in Egypt "unflavored (KasM) and peach flavored Moâssel (PFM)". Headspace GC-MS analysis allowed the identification of 52 compounds in the volatile profile of both samples with PFM more enriched with oxygenated compounds (72.71%), which made up of 34.23% in KasM profile. Alanine was the major identified compound in KasM (31.96%) *versus* linalool that was the most abundant constituent (48.16%) in PFM. Several potentially-health hazardous additives and toxic *de-novo* synthesized substances were also identified. Moreover, KasM and PFM methanol condensates were subjected to metabolomic profiling based on Liquid Chromatography High Resolution Electrospray Ionization Mass Spectrometry (LC-HR-ESI-MS), which showed the presence of a variety of unknown phytochemicals. The smoke obtained by a simulated Waterpipe smoking setup was subjected to pharmacological study using experimental animals to evaluate its toxicological impact on lung tissues. Pulmonary inflammation and increased oxidative stress was evidenced by increased levels of MDA and NO as well as histopathological changes in animal lung tissues.

Keywords

Moâssel; Headspace GC-MS; Metabolomic; LC-HR-ESI-MS analysis; Oxidative stress; MDA; NO; GSH.

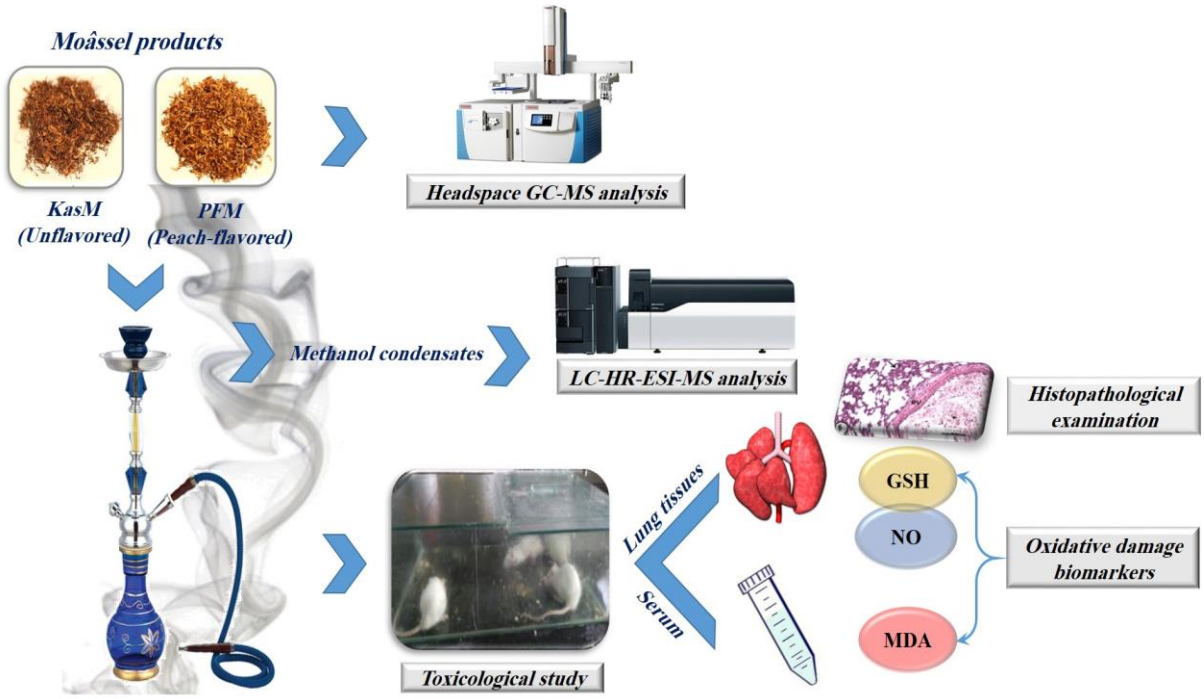

**** Correspondence:** Ashraf N. E. Hamed*
***Tel.:** +2086-234-77-59**; Fax:** +2086-236-90-75.*
***Email Address:** ashrafnag@mu.edu.eg*

1. Introduction

Tobacco use is an epidemic problem in today's society and the major leading cause of premature death in the United States amounting for 435,000 deaths annually. Attention has been shifted recently to a new trend into tobacco use, smoking tobacco using a Waterpipe or Hookah smoking [1]. The American Lung Association (ALA) and the World Health Organization (WHO) highlighted the increasing prevalence and untoward health effects of Waterpipe smoking among adolescents and young adults. These organizations have prescribed health warnings on its dangers [2].

Waterpipe smoking is a type of tobacco smoking and the most common type of tobacco used in the Waterpipe is called Moâssel, which is a mixture of crude fermented tobacco with molasses. The synthetic mixtures of volatile flavor compounds are usually added to imitate the respective natural flavor and to mask the bitterness of tobacco smoke compared to cigarettes, make it more appealing to users [1]. Waterpipe (syn.: Hookah; Shisha, Goza, Narghile, Arghile and Hubble bubble) is a pipe used to smoke a combination of tobacco, which is either flavored or unflavored. It consists of a head, body, bowl and hose with mouthpiece. Charcoal is often used for heated as the users inhale through the mouthpiece and hose and the mainstream smoke is produced and filtrated through water vessel [3].

The chemical composition of Moâssel of Waterpipe smoke, for a variety of smoking regimens, coal application schedules, and with or without water in the bowl was investigated [4].

The impact of the puffing regimen and coal application in "two apples" Nakhla Ma'assel, on the consumed tar, nicotine and tobacco was also investigated. Many adverse health effects have been reported including cardiovascular disease, cancer and addiction [5].

According to a WHO advisory, a typical one-hour session of Hookah smoking exposes the user to 100 to 200 times the volume of smoke inhaled from a single cigarette [6]. Hookah smoking is more harmful than cigarette smoking because even after the smoke passing through water vessel, it still contains high levels of the tobacco addictive substance “nicotine”, many toxic compounds such as carbon monoxide, heavy metals, carcinogens like tobacco specific nitrosamines, and different added Moâssel artificial flavoring substances [3].

However, little knowledge is available about the toxicological impact of these added flavors after being burnt by the Waterpipe smokers. Such relation needs to be explored as it is crucial for the assessment of potential health hazards associated with these additives.

Literature survey, six Egyptian flavoured Moâssel samples from Al Dandash company were chemically analysed by Headspace GC-MS *viz*., Apple, Creamy Strawberry, Mix Grapes, Guava, Mixed Fruits and Watermelon [7, 8].

Accordingly, the current study aimed to investigate the chemical constituents of more Waterpipe Moâssel products; “unflavored (KasM) and peach flavored Moâssel (PFM)” for their volatile profile by Headspace gas chromatography/mass spectrometry (Headspace GC-MS) as well as metabolomic profiling based on Liquid Chromatography High Resolution Electrospray Ionization Mass Spectrometry (LC-HR-ESI-MS). Furthermore, this study designed also to investigate the toxic effects of these Waterpipe Moâssel products by using a simulated smoking setup for Waterpipe.

2. Material and Methods

2.1. Moâssel products

Two Moâssel products KasM and PFM were produced by Al-Borg and Al-Dandash companies, respectively, were collected from the Egyptian market.

2.2. Extraction of Moâssel condensates

The methanol condensates of two Moâssel products were obtained after burning (Figure 1).

Figure 1: The Waterpipe simulated smoking setup before (**A**) and during burning (**B**) of the tested Moâssel products.

2.3. Chemical profile of Moâssel products

2.3.1. Headspace GC/MS analysis

The Moâssel products were subjected for Headspace GC-MS analysis. Shimadzu GC-MS with Headspace system provided by FID (Flame Ionization Detector), connected to the Mass Spectrometer Model: QP2010Ultra. Total GLC chromatograms and mass spectra were recorded in the electron impact ionization mode at 70 eV, using ACQ Mode of scan from 35 to 500 m/z in 0.3 sec. The used column was 0.25 mm in internal diameter, 30 m length, packed with Rtx-MS and 0.25 µm film thickness. The injected volume was 1.0 µl, using helium as carrier gas at flow rate 40 ml/min. The analysis was carried out at a programmed temperature; the initial temperature was 40 °C (Kept for 2 min), then increased at a rate 30-50 °C to the final temperature 210 °C (kept for 5 min). Injector and detector had the same temperature 230 °C. The total run time was 45 min and split ratio 1:50. Total ion chromatograms (TIC) and mass spectra were recorded in the electron impact ionization mode at 70 eV, using ACQ Mode of scan from 35 to 500 m/z in 0.3 sec [9].

2.3.2. Metabolomics analysis

Metabolite profiling was carried out on the methanol condensates of KasM and PFM using analytical techniques of LC-HR-ESI-MS [10]. Briefly, one mg of both condensates was dissolved in MeOH and then uploaded on an Accela HPLC (Thermo Fisher Scientific, Bremen, Germany) combined with Accela UV/VIS and Exactive (Orbitrap) mass spectrometer from Thermo Fisher Scientific (Bremen, Germany). The mobile phase composed of purified water (A) and acetonitrile (B) with 0.1% formic acid in each solvent. The gradient elution started at a flow rate of 300 µL/min with 10% B linearly increased to 100% B within 30 min and remained isocratic for the next 5 min before linearly decreasing back to 10% B for the following 1 min. The mobile phase was then equilibrated for 9 min before the next injection. The mass range was set from *m/z* (mass-to-

charge ratio) 100-2000 for ESI-MS using in-source CID (collision-induced dissociation) mechanism and *m/z* 50-1000 for MS/MS using untargeted HCD (high energy collision dissociation). The raw mass spectrometry data were imported to MZmine 2.12 for chromatogram deconvolution and peaks deisotoping. The retention time normalizer was applied for chromatographic alignment and gap-filling. Excel macros were used to combine positive and negative ionization mode data files generated by MZmine. Peaks were then extracted and Excel macro was used to dereplicate each *m/z* ion peak with compounds in the customized database (using RT and *m/z* threshold of ±5 ppm). A detailed putative identification of all metabolites in the total extract was provided. The macro was then utilized to identify the top 20 features (ranked by peak intensity) and the corresponding putative identities by creating a list for the methanol condensates. The burned compounds were identified by comparison with some online and in-house databases.

2.4. Experimental animals

Forty-five adult male albino rats of (150±20 g) were used throughout the experiments. Animals were housed under standard 12 h light/dark cycle, fed with standard rat chow diet and tap water *ad libitum* and left to acclimatize to the environment for one week prior to initiation of the experiment. Experiments were conducted in accordance with the international ethical guidelines for animal care of United States Naval Medical Research Center, Unit No. 3, Abbaseya, Cairo, Egypt, accredited by the Association for Assessment and Accreditation of Laboratory Animal Care International (AAALAC). Ethical clearance for performing the experiments on animals was obtained from of "The Research Ethics Committee", Faculty of Pharmacy, Minia University, Egypt No. 018/17. The adopted guidelines are in accordance with "Principles of Laboratory Animal care" (NIH publication No. 85/23, revised 1985).

2.5. Animal exposure to Waterpipe Moâssel smoke

Waterpipe simulated smoking setup was assembled as a glass chamber in which its dimensions were 90 cm length x 50 cm width x 30 cm height. It has two opens; one connected to a pump (for smoke suction), while the second open connected with Waterpipe (in which Moâssel was burnt using charcoal). The generating smokes and normal airs were introduced to the glass chamber *via* a custom-made 3-way valve. The smoking cycle was composed of 15 sec smoke followed by 20 sec normal air. Before the smoke exposure, vaseline was used during the experiment to improve the pump suction. The tested animals were divided into three groups: control (no smoke), PFM and KasM, each containing 15 rats. The rats in both PFM and KasM groups were divided into three subgroups, each containing 5 rats. Each subgroup (5 rats) was exposed to the generated smoke for different exposure time *i.e.* 5, 10 and 15 min (Figure 2).

Figure 2: The glass chamber for Waterpipe simulated smoking setup.

2.6. Histopathological examination

Lung tissues were fixed in 10% PBS-buffered formalin solution for 24 h, followed by decalcification in formic acid. Samples were washed in tap water then dehydrated by absolute ethanol. Samples were cleared in xylene and embedded in paraffin at 56 °C in hot air oven for 24 h. Paraffin-beeswax tissue blocks were prepared for sectioning at 4 μm thickness with a sledge microtome. The obtained tissue sections were collected on glass slides, de-paraffinized, stained with Hematoxylin & Eosin stain (H&E) then examined under a light microscope [(Leica® Model DM 1000 (US listed microscope)] equipped with a camera (Leica®, EC3, Switzerland).

2.7. Preparation of lung tissue and homogenate

At the end of the experimental protocol, thoraces were rapidly cut, open, and lung tissue samples were harvested immediately after animal sacrifice. Tissues were washed in cold phosphate buffered saline (PBS, pH 7.4) to make sure it is free of residual blood and connective tissue, and blotted dried on a filter paper. Immediately, tissue samples were flash-frozen in liquid nitrogen and kept frozen at -80 °C until the time of analysis.

Prior to analysis, lung tissues of known weight were homogenized for 10 min in PBS, pH 7.4 (10% W/V), using a motor driven homogenizer (Heidolph, Germany) in an ice bath. Homogenates were further centrifuged for 10 min at 10000 rpm and the supernatant was separated for use in subsequent analyses. In addition, other samples of lung tissue from each group were collected for routine histological assessment of lung injury [11].

2.8. Determination of oxidative stress biomarkers

2.8.1. Assay of malondialdehyde (MDA) content

Lipid peroxidation products such as malondialdehyde (MDA) were determined as a marker of oxidative stress. MDA was determined in the lung tissues as thiobarbituric acid-reactive-substances (TBARS). The principle of the assay depends on the derivatization of MDA (one of the lipid peroxidation products) with thiobarbituric forming a pink colored adduct. The absorbance of the adduct was then evaluated spectrophotometrically according to a previously described method [12].

2.8.2. Assay of total nitrate/nitrite content

Nitrate and nitrite were assayed colorimetrically as indicators of nitric oxide (NO) in the tissue because the half-life of NO is too short and it is proportionately converted into nitrite and nitrate. The total of nitrate/nitrite (Total NO) in the sample was assayed as nitrite after reduction of nitrate into nitrite using the cadmium reduction method. Then the total nitrite was measured by employment of the Griess reaction via a diazotization reaction followed by photometric quantization of the formed azodye at 545 nm [13].

2.8.3. Assay of reduced glutathione (GSH) content

The method is based on the reduction of DTNB (5,5'-dithiobis-(2-nitrobenzoic acid) by GSH giving a yellow compound measured at 405 nm. The concentration of the reduced

chromogen is directly proportional to the sample GSH concentration [14].

2.9. Statistical analysis

Data was analyzed using the Graphpad Prism®5.0 (Graphpad Software, San Diego, California, USA). The results were expressed as mean±S.E.M. Statistical significance was determined using one-way analysis of variance (ANOVA) followed by Tukey's multiple comparison test, values of $p<0.05$ indicated statistical significance.

3. Results and Discussion

3.1. Headspace GC-MS of KasM and PFM

Identification of the volatile components in KasM and PFM was carried out by direct comparison of retention time (Figure 3) and fragmentation pattern of each of the identified compounds and quantitation was based on peak area integration [15]. The GC-MS identified compounds are listed in (Tables 1 and 2). The volatile profile of the KasM sample smoke contained thirty volatile compounds belonging to two major classes *viz.* oxygenated and nitrogenous compounds totaling 56.26 and 34.23%, respectively (Table 1). However, only twenty-three volatile compounds were identified in the flavored Moâssel (PFM) mostly oxygenated compounds amounted for 72.71% of the identified compounds (Table 2). The structures of some detected compound are demonstrated in Figure 4.

Both chromatograms have only one common peak corresponding to furfural, a natural compound produced as a result of dehydration of pentose sugar, which is of particular importance being considered as a main contributor to the toxicity of hemicellulose syrups and increases the toxicity of other compounds [16]. It is present in higher concentration (3.16%, compared to 0.82% present in PFM) in KasM, which contained also its less toxic alcohol counterpart. Furfural has been reported to alter DNA structure and sequence [17] and slow down sugar metabolism [18]. 5-Methyl-2-furfural and 5-hydroxymethyl-2-furfural together acetone was reported only after re-drying and aging of Moâssel. These compounds were identified only in the chromatographic profile of KasM sample, which suggest that aged raw material was used for its manufacture [19].

Alanine is the major compound amounting for 31.96% of the total monitored peaks, which is an α-amino acid used in protein biosynthesis. In mammals, it plays a key role in glucose-alanine cycle between tissue and liver [20]. The alternation in this cycle increases the level of serum alanine aminotransferase (ALT) that is linked to the incidence of type 2 diabetes [21].

Nicotine is recorded only in GC/MS chromatogram of the KasM sample in a concentration of 2.27%. Despite being presumed to be the main addictive component in Moâssel smoke, it was corroborated that other constituents in Moâssel smoke contribute to its addictive properties [22]. Among these Moâssel constituents, acetaldehyde was only identified in KasM smoke in a concentration of 2.20%. This aldehydic compound was previously reported to be one of the major components in Moâssel smoke produced as a result of polysaccharides combustion [23]. Its presence in low concentration in mainstream smoke was reported to synergistically enhance the reinforcing effects of nicotine. The addictive potential acetaldehyde is believed to be initiated *via* salsolinol and harman, condensation products formed from acetaldehyde and biogenic amines, both during Moâssel smoking and *in-vivo*, which inhibit monoamine oxidase and hence, increasing behavioral sensitization to nicotine. This suggests that the administration of antidepressants might be an efficient strategy in quit smoking programs to compensate for the pharmacological effects of acetaldehyde-biogenic amine condensation products [22].

The volatile profile of KasM also contained acetic acid, most probably formed by pyrolysis, in a moderate abundance (10.53% of the identified compounds), which was documented to cause a mild nasal irritation at 10 ppm [24].

Diethyl phthalate is most probably appeared in PFM due to its common use as a solvent and vehicle for fragrances and other cosmetics ingredients despite having some environmental and human health concerns [25].

Regarding PFM sample, linalool was the major identified compound making up to 48.16% of the total compounds. Linalool is a monoterpene found abundantly in the essential oils of several aromatic plants, which are used as sedative in traditional herbal medicine. Its inhalation caused allergic reactions, irritation, drowsiness or dizziness and potentially unsafe to the unborn child [26]. It was reported to possess acute oral mammalian LD_{50} of 3 g/kg bw and acute dermal toxicity ≥ 2 g/kg b.w. [27]. Linalool oxide is also present in KasM sample but in much lower abundance. Its inhalation was reported to exert an anxiolytic effect in experimental animals, without causing any motor impairment [28].

Glycerol has been identified in 0.2% of the total profile, which was reported to be Moâssel as humectants which are easily carried into the mainstream smoke [19].

A series of damascone isomers were identified making up to 3.15% of the identified volatile components. These compounds belong to a class of chemicals known as rose ketones produced as a result of carotenoids degradation, which also includes damascenones and ionones. (*E*) β-Damascone is the main contributor to the aroma of roses, despite its low abundance in the essential oil of roses. Similarly, it is present in KasM sample profile in the lowest concentration of 0.23% among the other damascones [29]. (*E*) β-Damascone was also reported to be produced from β-ionone, cyclic terpenoid derivatives with violet-like odor, that occur in many essential oils, through its reduction into β-ionol, which undergoes an oxygenase-induced conversion into theallenic diol and the latter is rearranged into (*E*) β-damascone. As early as 1971 both compounds (*E*) β-damascone and β-ionone were isolated from tobacco [30]. It is worth noting here that γ-decalactone (2.59%) has a fruity, peach-like odor with an aroma which is used in perfumery to produce peachy flavors. α-Terpineol is one of the most commercially important monoterpene alcohol with a lilac odor and sweet smell reminiscent of peach [31].

3-Hexen-1-ol, being present in a concentration of 9.55%, was reported to be added to cigarette tobacco to enhance its organoleptic properties and to impart the characteristic smell of newly mown grass [32].

The occurrence of such a wide range of volatile flavor compounds in Moâssel, including allergenic fragrances, *i.e.* benzyl alcohol, which constituted about 0.24% of the volatile profile of PFM, might pose a potential health risk to the smoker. Some of these flavoring compounds could be precursors for toxic compounds upon heating [33].

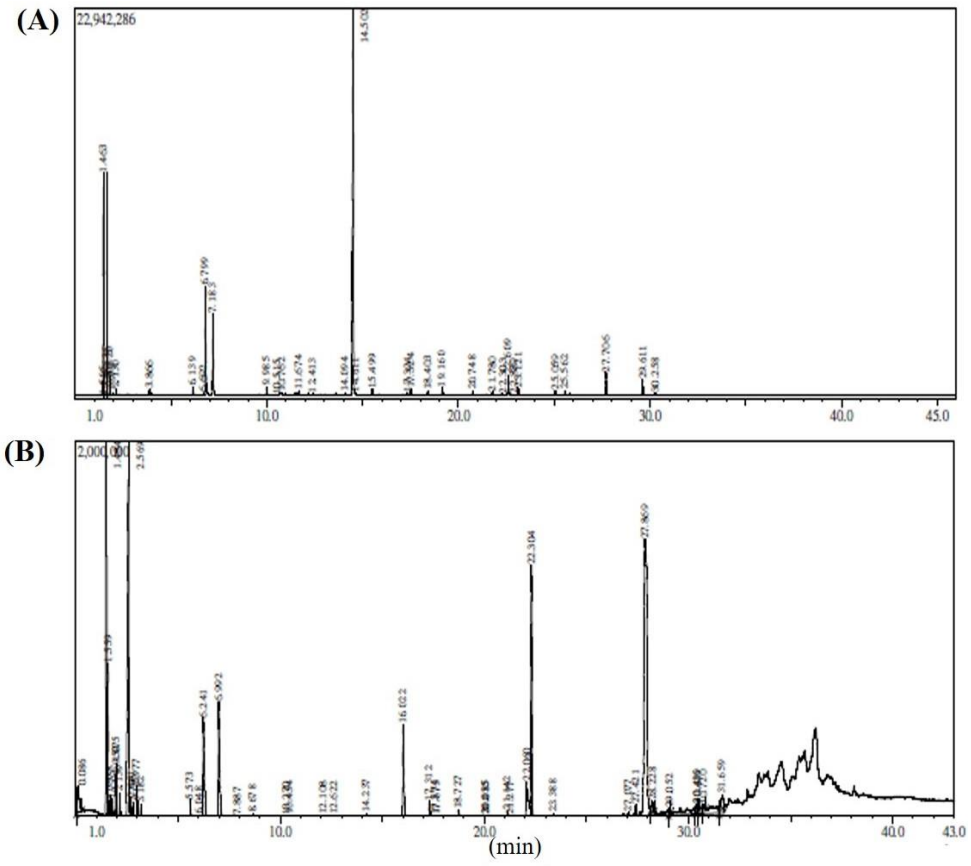

Figure 3: GC-MS total ion chromatograms of (**A**) KasM and (**B**) PFM.

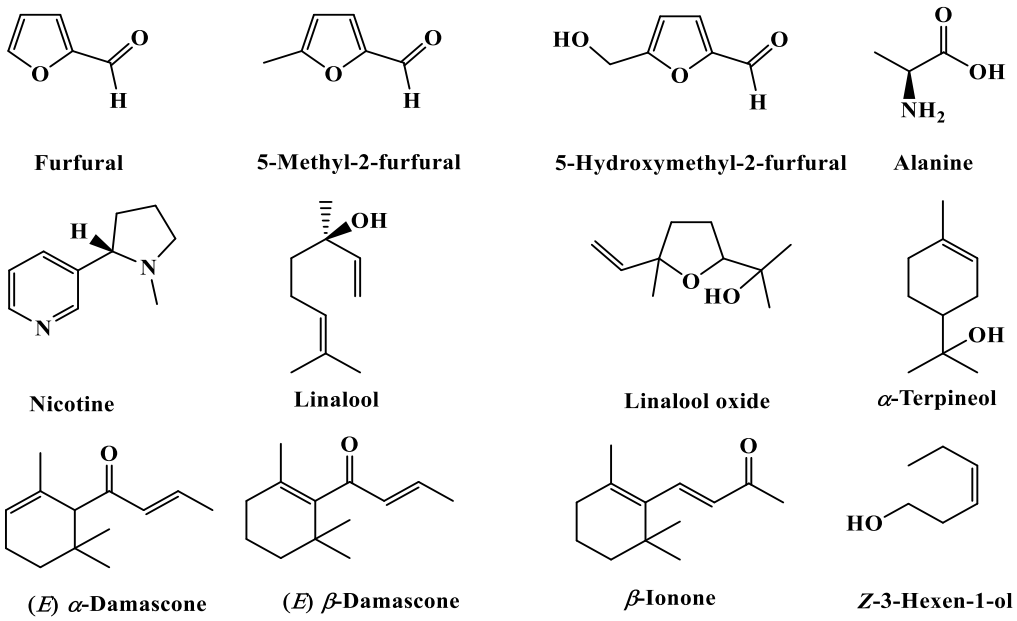

Figure 4: Chemical structures of some identified compounds discussed throughout the manuscript.

Table 1: The identified compounds in KasM by Headspace GC-MS.

No.	Name	RT*	RRT**	Base peak	Relative Area %	M. Weight	M. Formula
1	*E*-2-Dodecenyl acetate	00.09	00.057	43	01.52	226	$C_{14}H_{26}O_2$
2	Alanine	01.48	01.000	44	31.96	89	$C_3H_7NO_2$
3	Acetaldehyde	01.56	01.054	44	02.20	44	C_2H_4O
4	Ethanol	01.67	01.128	45	00.39	46	C_2H_6O
5	Acetone	01.77	01.195	43	00.28	58	C_3H_6O
6	Formic acid	01.95	01.317	46	00.39	46	CH_2O_2
7	2-Methylpropanol	01.97	01.331	43	00.73	74	$C_4H_{10}O$
8	2,3-Butanedione	02.14	01.445	43	00.30	86	$C_4H_6O_2$
9	Acetic acid	02.57	01.736	43	10.53	60	$C_2H_4O_2$
10	3-Methylbutanal	02.67	01.804	43	00.26	86	$C_5H_{10}O$
11	2-Methylbutanal	02.79	01.885	41	00.24	86	$C_5H_{10}O$
12	Hydroxyacetone (syn.: 1-hydroxy-2-propanone)	02.97	02.006	43	01.04	74	$C_3H_6O_2$
13	2,3-Pentanedione	03.18	02.148	43	00.26	100	$C_5H_8O_2$
14	Dihydro-2-methyl-3-furanone	05.57	03.763	43	00.84	100	$C_5H_8O_2$
15	Butanoic acid	06.05	04.087	60	00.17	88	$C_4H_8O_2$
16	Furfural	06.24	04.216	96	03.16	96	$C_5H_4O_2$
17	Furfuryl alcohol	06.99	04.722	98	03.74	98	$C_5H_6O_2$
18	2-Cyclopentene-1,4-dione	07.88	05.324	96	00.22	96	$C_5H_4O_2$
19	2-Acetylfuran	08.68	05.864	95	00.38	110	$C_6H_6O_2$
20	5-Methyl-2-furfural	10.27	06.939	110	00.27	110	$C_6H_6O_2$
21	Hydroxyethyl methylacrylate	12.10	08.175	69	00.31	130	$C_6H_{10}O_3$
22	Phenylacetaldehyde	12.62	08.527	91	00.21	120	C_8H_8O
23	Methyl benzoate	14.23	09.614	105	00.35	136	$C_8H_8O_2$
24	3-Hydroxy-2,3-dihydromaltol	16.02	10.824	43	03.49	144	$C_6H_8O_4$
25	Menthyl acetate	17.57	11.871	43	00.20	198	$C_{12}H_{22}O_2$
26	5-Hydroxymethyl-2 furaldehyde	18.72	12.648	97	00.63	126	$C_6H_6O_3$
27	Nicotine	22.06	14.905	84	02.27	162	$C_{10}H_{14}N_2$
28	Spathulanol	27.07	18.290	43	00.19	220	$C_{15}H_{24}O$
29	Isospathulenol	27.42	18.527	43	00.53	220	$C_{15}H_{24}O$
30	Diethyl phthalate (syn.: Solvanol)	27.86	18.820	149	23.43	222	$C_{12}H_{14}O_4$
Unidentified compounds 09.51%							
Identified compounds 90.49%		Oxygenated compounds 56.26%					
		Nitrogenous compounds 34.23%					

*RT: Retention Time. **RRT: Relative Retention Time.

Table 2: The identified compounds in PFM by Headspace GC-MS.

No.	Name	RT*	RRT**	Base peak	Relative Area %	M. Weight	M. Formula
1	Isobutanal	01.97	0.136	43	0.45	72	C_4H_8O
2	Isoamyl alcohol	03.80	0.262	55	0.41	88	$C_5H_{12}O$
3	Furfural	06.14	0.423	96	0.82	96	$C_5H_4O_2$
4	*Z*-3-Hexen-1-ol	06.80	0.469	41	9.55	100	$C_6H_{12}O$
5	Benzaldehyde	09.98	0.688	77	0.82	106	C_7H_6O
6	Glycerol	10.51	0.725	61	0.20	92	$C_3H_8O_3$
7	*n*-Hexyl acetate	11.67	0.805	43	0.39	144	$C_8H_{16}O_2$
8	Benzyl alcohol	12.40	0.855	79	0.24	108	C_7H_8O
9	Linalool oxide	14.09	0.972	59	0.28	170	$C_{10}H_{18}O_2$
10	Linalool	14.50	1.000	71	48.16	154	$C_{10}H_{18}O$
11	Dihydrolinalool	15.50	1.069	109	0.59	156	$C_{10}H_{20}O$
12	α-Terpineol (syn.: Menth-1-en-8-ol)	17.32	1.194	59	0.30	154	$C_{10}H_{18}O$
13	Ethyl maltol	17.52	1.208	140	0.72	140	$C_7H_8O_3$
14	Nerol	18.40	1.269	69	0.46	154	$C_{10}H_{18}O$
15	2-Methyl cylohexane-1,4-dione	20.75	1.431	126	0.36	126	$C_7H_{10}O_2$
16	Benzyl butanoate	21.78	1.502	91	0.34	178	$C_{11}H_{14}O_2$
17	*E*-α-Damascone	22.60	1.559	69	2.14	192	$C_{13}H_{20}O$
18	*E*-β-Damascone	22.88	1.578	69	0.23	192	$C_{13}H_{20}O$
19	*Z*-α-Damascone	23.12	1.594	69	0.78	192	$C_{13}H_{20}O$
20	γ-Decalactone	25.06	1.728	85	0.68	170	$C_{10}H_{18}O_2$
21	β-Ionone	25.56	1.763	177	0.51	192	$C_{13}H_{20}O$
22	γ-Undecalactone	27.70	1.910	95	2.59	184	$C_{11}H_{20}O_2$
23	Dihydro methyl jasmonate	29.61	2.042	83	1.69	226	$C_{13}H_{22}O_3$
Unidentified compounds 27.29%							
	Identified oxygenated compounds 72.71%						

*RT: Retention Time. **RRT: Relative Retention Time.

3.2. Metabolomics profiling of KasM and PFM

The methanol condensates of KasM and PFM were subjected to metabolomic analysis using analytical techniques of LC-HR-ESI-MS according to Mahmoud et al., 2019 [34]. Metabolomic profiling resulted in the characterization of a variety of constituents (Figures 5-7 and Tables 3&4) with several unidentified compounds. One of tentatively identified compounds (3,5-Dichloroaniline) was reported to produce methemoglobinemia in rats & mice when administered intraperitoneally at a dose of 0.8 mmol/kg [35] besides, it was nephrotoxic to Sprague Dawley rats, when administered at a dose of 0.8 mmol/kg or higher due to its ability to alter organic ion transport in the rats [36]. 3,5-Dichloroaniline had a higher nephrotoxic potential than its (2,4-), (2,6-) and (3,4-) analogues [37].

However, resorcinol has a well-documented peroxidases inhibition activity in the thyroid due to its ability to block the synthesis of thyroid hormones causing goiter and interfere with the iodination of tyrosine and the oxidation of iodide [38, 39]. Most importantly, benzo(α)pyrene is reported to be contained in gasoline and diesel exhaust, cigarette smoke, coal tar and coal tar pitch, which is proved to be a potential human carcinogen [40].

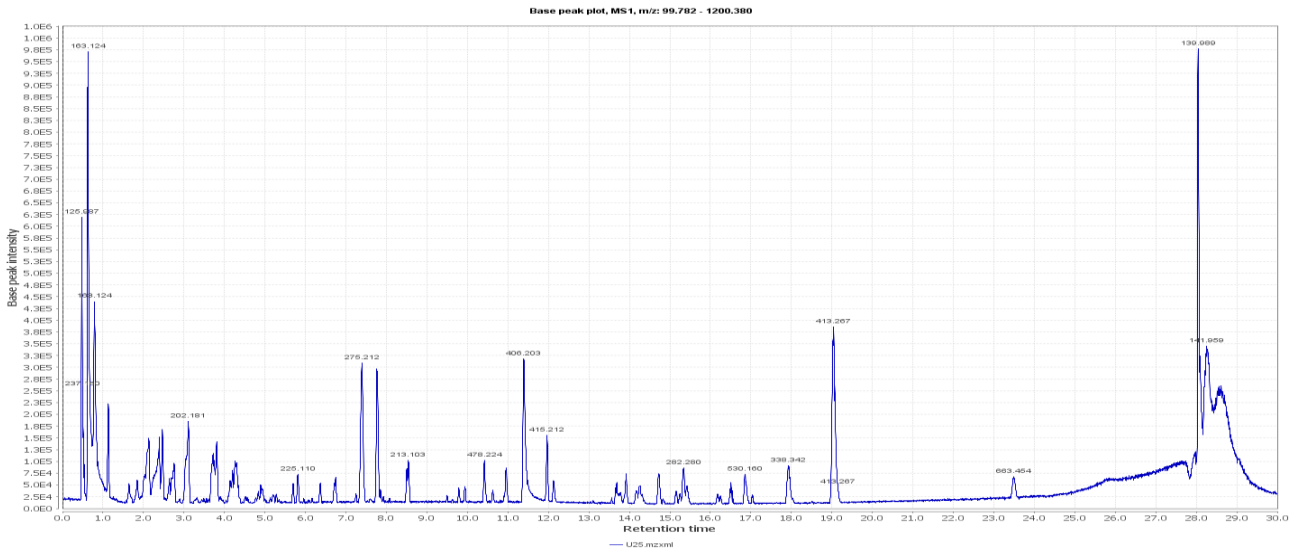

Figure 5: Total ion chromatograms of KasM methanol condensate.

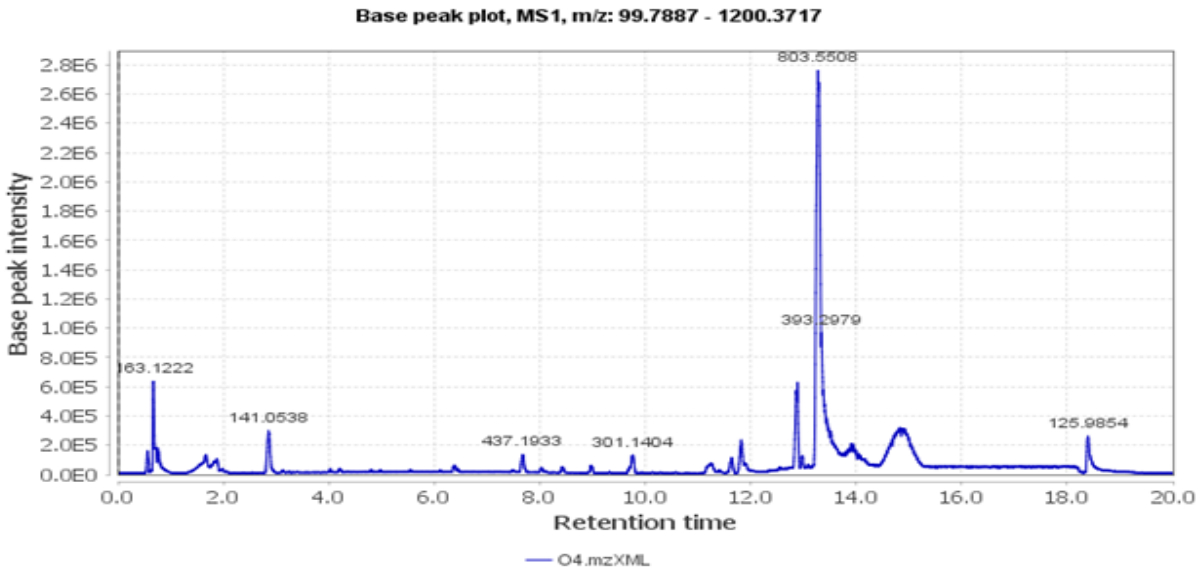

Figure 6: Total ion chromatogram of PFM methanol condensate.

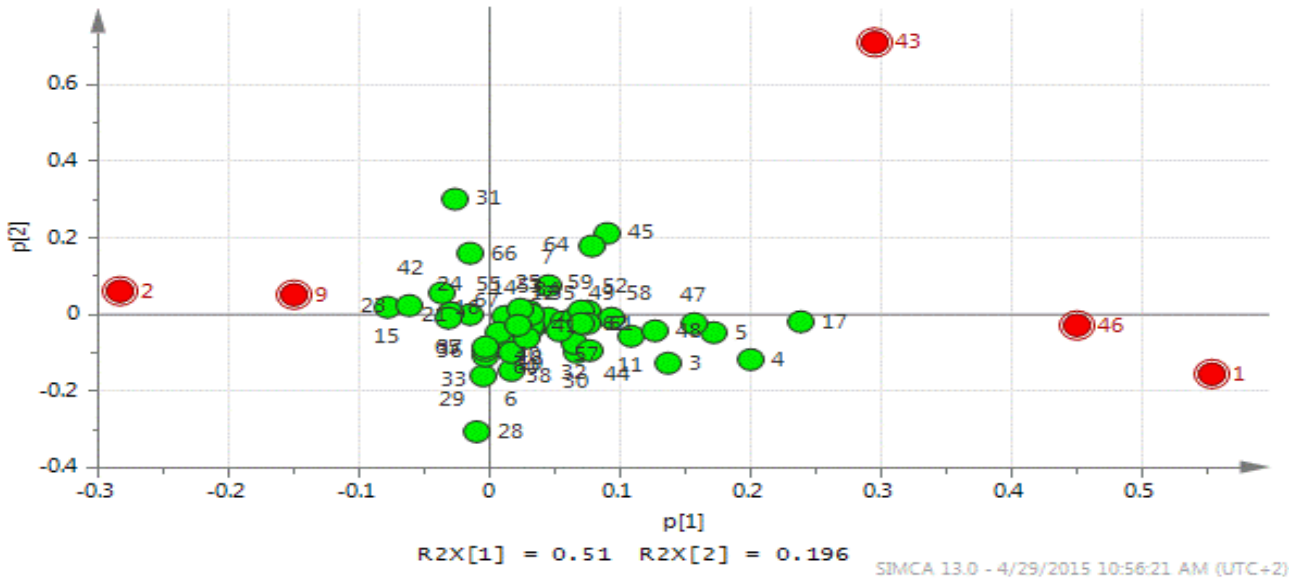

Figure 7: SIMCA plot showing the outlying masses (compound masses).

Table 3: The outlying masses and their predicted compounds of KasM.

Var ID (Primary)	Predicted compound	Var ID (row retention time)	Var ID (row m/z)
2	Unknown	28.1727	141.988
6	Unknown	19.0457	413.267
17	Unknown	00.8427	163.123
18	Unknown	28.2243	141.959
19	Unknown	03.1826	202.181
20	Unknown	00.8002	132.081
21	Unknown	28.1874	128.951
22	Unknown	01.5574	223.058
23	Unknown	02.2360	130.159
25	Unknown	01.9299	127.039
26	Unknown	15.4183	270.280
27	Unknown	01.7617	183.066
28	Unknown	28.1498	110.020
30	Unknown	28.0638	141.987

Table 4: The outlying masses and their predicted compound of PFM.

Var ID (Primary)	Predicted compound	Var ID (row m/z)	Var ID (MS)
1	Unknown	13.28	412.259
2	Unknown	13.31	392.290
9	Unknown	13.31	762.599
43	Unknown	14.73	505.522
46	Unknown	13.15	802.537
6	3,5-Dichloroaniline	01.99	162.017
10	Resorcinol	00.56	110.111
33	3-Biphenylamine	03.09	169.089
34	Benzo(α)pyrene	12.87	252.309
44	Qunioline	02.80	129.058

3.3. Toxicological impact of the Waterpipe smoke of KasM and PFM

A second goal of our study was to evaluate the toxicological impact of exposure to the smoke generated from KasM and PFM. Histopathological as well as biochemical examination of lung tissues of the two groups of rats exposed to the smoke was conducted.

It was found that exposure to Waterpipe smoke at different exposure times led to pulmonary inflammatory changes manifested as a gradual loss of normal lung architecture with an increase in the thickening of interalveolar septa and arterial wall and interstitial cellular infiltration as the time of exposure increases as shown in (Figure 8).

3.4. Biochemical assessment of relation between Waterpipe smoke exposure and oxidative stress in lungs

The observed pulmonary inflammation as a result of smoke exposure is expected to be due to the disturbed oxidant/antioxidant balance caused by the oxidative stress resulting from the high amounts of oxygen-derived species and free radicals in Waterpipe smoke. Accordingly, oxidative stress biomarkers indicative of lung tissue toxicity such as lipid peroxidation (MDA) and increased reactive nitrogen species (total nitrite content) were determined. In addition, tissue level of reduced glutathione (a protective marker) was also assessed and summarized the effect of Waterpipe smoke exposure on the three assessed biomarkers of oxidative stress (MDA, NO, and GSH) in experimental animals (Table 5).

Table 5: The estimated levels of MDA, NO and GSH in the control and exposed groups to smoke of KasM and PFM at 5, 10 and 15 min of exposure.

Group	MDA (nmole/ml)	NO (nmole/mg)	GSH (nmole/mg)
Control	44.60±2.422	8.23±0.72	0.25±0.034
KasM5	52.81±1.140	10.92±0.58	0.39±0.028
KasM10	60.00±5.170	12.07±0.56	0.47±0.072
KasM15	89.36±9.380*	18.26±1.37*	0.54±0.110
PFM5	72.38±6.770	15.41±1.32*	0.55±0.027
PFM10	65.91±3.710	14.72±0.74*	0.48±0.030
PFM15	56.78±4.350	13.08±0.36*#	0.42±0.080

Data represent the mean±SE

*Significant difference from control group at $p<0.05$.

Significant difference from KasM15 (group exposed to KasM for 15 min) at $p<0.05$).

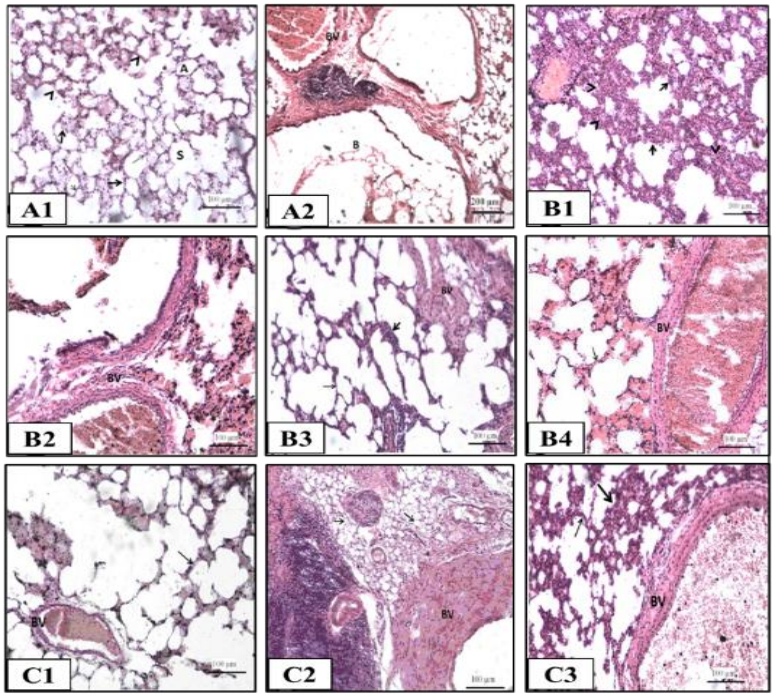

Figure 8: Representative photomicrograph of histological sections of the lung of (**A1**&**A2**) control group, **a:** normal lung architecture with clear alveoli [**A**], alveolar sacs [**S**], thin interalveolar septa [➢], type I flattened pneumocyte [➔] and type II cuboidal pnemocyte [➔] lining the spaces. **b:** bronchioles [**B**] and blood vessels [**BV**]; (**B1**&**B2**) rat groups exposed to Waterpipe smoke of PFM for: 5 min (**B1**&**B2**), **a:** thickened interalveolar septa [➔] with massive interstitial cellular infiltration [➢] and loss of normal architecture. **b:** The arterial wall is hypertrophied to some extent (**BV**), 10 min (**B3**) the lung architecture appears more or less normal with thin interalveolar septa in some areas [➔] and thickened infiltrated with inflammatory cells in other areas [➔] and thickened arterial wall is still seen [**BV**] and 15 min (**B4**) the lung architecture nearly similar to the previous group, interalveolar septa [➔] and blood vessel [**BV**] were seen and (C) rat groups exposed to Waterpipe smoke of KasM for: 5 min (**C1**) normal lung architecture with thin interalveolar septa [➔] and normal blood vessel [**BV**], 10 min (**C2**) thin interalveolar septa [➔] and very thick arterial wall [**BV**] and 15 min (**C3**) thin interalveolar septa in some areas [➔] and thickened infiltrated with inflammatory cells in other areas [➔]. The arterial wall is thickened to some extent [**BV**], **H&E X 400**.

3.4.1. Effect of Moâssel smoking on lung tissue MDA level

Animals exposed to either Waterpipe smoke of KasM or PFM were found to have greater MDA values than the control group (44.60±2.422 nmol/ml), in most of the applied exposure times. In addition, the KasM smoke-exposed animals showed an exposure time-dependent increase in MDA level. On the contrary, animals exposed to PFM smoke showed a surprisingly reversed pattern, *i.e.*, smaller values were observed with increasing the time of exposure.

3.4.2. Effect of Moâssel smoking on lung tissue total nitrate/nitrite level

The animal lungs exposed to KasM and PFM smoke had higher total nitrate/nitrite values than control animals (8.23±0.72 nmol/mg), indicating greater levels of biological stress after smoke exposure. Not surprisingly, the animals exposed to KasM showed an increase in the value of NO metabolite concentrations, which was parallel to the increase in time of exposure, *i.e.*, KasM15 min showed NO values greater than in the KasM5 min group. On the other hand, the PFM exposed animals showed smaller values with increased exposure time.

3.4.3. Effect of Moâssel smoking on lung tissue reduced GSH concentration

The levels of reduced glutathione (GSH) in lungs of the animals exposed to either KasM or PFM have greater values than the control (0.25±0.034 nmol/g). The KasM smoke-exposed animals showed a trend of increasing GSH values in response to exposure time, whereas, an opposite trend was observed in the PFM smoke-exposed animals.

Overall, the results showed that animal exposure to smoke was inferior to breathing of normal air in the control group, as would be expected. In addition, smoking KasM resulted in exposure-time-dependent deterioration in lung biochemical parameters, which was confirmed by the results obtained by lung histological investigation.

On the other hand, the PFM group showed moderate (less severe) results, when compared to KasM groups. These findings are in agreement with previous results reported by Shraideh and Najjar 2011 [41], where significant structural changes, which are expected to affect lung function, were observed in alveolar histology [42]. However, the usefulness of their results is limited by the fact that they only studied the effects of smoking on pulmonary histology. This limitation was addressed by the current work as we also measured biochemical changes that were directly correlated with smoking-induced structural changes. Indeed, our biochemical parameters are in line with the histological changes observed in the lung tissues (increased MDA and NO as directly correlated with higher magnitudes of lung damage). These findings are in agreement with the results published by Shraideh and Najjar 2011 [41].

On the other hand, the paradoxical changes in reduced GSH levels might be explained as a compensatory defensive mechanism, or as a direct effect of the smoke constituents; either of which couldn't be ruled out by the results of this study.

Conclusion

Several hazardous additives including allergenic fragrances, *i.e.* benzyl alcohol and linalool, in addition to *de novo* synthesized substances, such as toxic dehydration product of sugars, *i.e.* furfural, and polysaccharides combustion product with addictive potential *i.e.* acetaldehyde, were identified in the volatile profile of two Moâssel products by Headspace GC-MS analysis. These compounds may pose potential health risk to smokers whether being toxic by its own or precursors for other hazardous substances upon heating. Further toxicological investigation of their individual effect is yet to be conducted.

Moreover, based on the presence of acetone, 5-methyl-2-furfural and 5-hydroxymethyl-2-furfural in KasM, it was possible to identify it as being manufactured from re-dried and aged raw material.

The association between Waterpipe Moâssel smoke exposure and oxidative stress in lungs was verified by the recorded deterioration in lung biochemical parameters, *i.e*. increased levels of oxidative stress biomarkers, *viz.* MDA and NO in experimental animals exposed to Waterpipe smoke. This was in alignment with the pulmonary inflammatory changes observed in lung histopathology. The current results provide experimental evidence that adds further knowledge on the health consequences of smoking Waterpipe.

Acknowledgment

We are deeply thankful to Prof. Dr. Rasha Ibrahim Anwar, Department of Anatomy, Faculty of Medicine, Assiut University, for her great help in carrying out the histopathological studies.

Conflict of interests

No potential conflict of interest was reported by the authors.

Orcid

Ashraf N. E. Hamed orcid.org/0000-0003-2230-9909

References

[1] Shihadeh A. Investigation of mainstream smoke aerosol of the argileh water pipe. *Food and Chemical Toxicology*. 2003;41:143-52.

[2] American Lung Association. an Emerging Deadly Trend: Waterpipe Tobacco Use. *Tobacco Policy Trend Alert*. 2007;1-9.

[3] Maziak W, Ward KD, Afifi Soweid RA, Eissenberg T. Tobacco smoking using a waterpipe: A re-emerging strain in a global epidemic. *Tobacco Control*. 2004;13(4):327-33.

[4] Shihadeh A, Saleh R. Polycyclic aromatic hydrocarbons, carbon monoxide, "tar", and nicotine in the mainstream smoke aerosol of the narghile water pipe. *Food and Chemical Toxicology*. 2005;43:655-61.

[5] Shihadeh A, Azar S, Antonios C, Haddad A. Towards a topographical model of narghile water-pipe café smoking: A pilot study in a high socioeconomic status neighborhood of Beirut, Lebanon. *Pharmacology Biochemistry and Behavior*. 2004;79:75-82.

[6] World Health Organization. TobReg Advisory Note - Waterpipe Tobacco Smoking: Health Effects, Research Needs and Recommended Actions by Regulators, WHO. 2005.

[7] Ismail MM., Hamed ANE, Fouad MA, Kamel MS. Comparative Head Space GC/MS Studies of Different Flavoured Moàssel in the Egyptian Market (I). *International Journal of Pharmacognosy and Phytochemical Research*. 2018;10(3):116-22.

[8] Ismail MM., Hamed ANE, Fouad MA, Kamel MS. Comparative Head Space GC/MS Studies of Different Flavored Moâssel in the Egyptian Market (II). *Journal of Advanced Biomedical and Pharmaceutical Sciences*. 2019;2(3):77-82.

[9] Hamed ANE, Abdelaty NA, Attia EZ, Desoukey SY. Phytochemical investigation of saponifiable matter & volatile oils and antibacterial activity of *Moluccella laevis* L., family Lamiaceae (Labiatae). *Journal of Advanced Biomedical and Pharmaceutical Sciences*. 2020;3(4):213-20.

[10] Abdelmohsen UR, Cheng C, Viegelmann C, Zhang T, Grkovic T, Ahmed S, Quinn RJ, Hentschel U, Edrada-Ebel RA. Dereplication strategies for targeted isolation of new antitrypanosomal actinosporins a and B from a marine sponge associated-Actinokineospora sp. EG49. *Marine Drugs*. 2014;12:1220-44.

[11] Downie T. Theory and Practice of Histological Techniques Edited by J.D. Bancroft & A. Stevens, Churchill Livingstone, Edinburgh. *Histopathology*. 1990;17(4):386.

[12] Samy MN, Hamed ANE, Mahmoud BK, Attia EZ, Abdelmohsen UR, Fawzy MA, Attya ME, Kamel MS. LC-MS based identification of bioactive compounds and hepatoprotective and nephroprotective activities of *Bignonia binata* leaves against carbon tetrachloride induced injury in rats. *Natural Product Research (Formerly Natural Product Letters)*. 2021:1-5. https://doi.org/10.1080/14786419.2021.1873982

[13] Sun J, Zhang XJ, Broderick M, Fein H. Measurement of nitric oxide production in biological systems by using Griess Reaction assay. *Sensors*. 2003;3:276-84.

[14] Hamed ANE, Wahid A. Hepatoprotective activity of *Borago officinalis* extract against CCl_4-induced hepatotoxicity in rats. *Journal of Natural Products (Indian)*. 2015;8:113-22.

[15] The National Institute of Standards and Technology. NIST/EPA/NIH Mass Spectral Library (NIST 08) and NIST Mass Spectral Search Program (Version 2.0f) User's Guide. Natl. Inst. Stand. Technol. NIST 2004;1-49.

[16] Zaldivar J, Martinez A, Ingram LO. Effect of selected aldehydes on the growth and fermentation of ethanologenic *Escherichia coli*. *Biotechnology and Bioengineering*. 1999;65:24-33.

[17] Khan QA, Shamsi FA, Hadi SM. Mutagenicity of furfural in plasmid DNA. *Cancer Letters*. 1995;89(1):95-9.

[18] Hristozova T, Angelov A, Tzvetkova B, Paskaleva D, Gotcheva V, Gargova S, Pavlova K. Effect of furfural on carbon metabolism key enzymes of lactose-assimilating yeasts. *Enzyme Microbial Technology*. 2006;39(5):1108-12.

[19] Johnstone RAW, Plimmer JR. The Chemical Constituents of Tobacco and Tobacco Smoke. *Chemical Reviews*. 1959;59(5):885-936.

[20] Nelson D, Cox M. Lehninger principles of biochemistry (4th ed.). *Biochemistry and Molecular Biology Education*. 2005.

[21] Sattar N, Scherbakova O, Ford I, O'Reilly DSJ, Stanley A, Forrest E, MacFarlane PW, Packard CJ, Cobbe SM, Shepherd J. Elevated alanine

aminotransferase predicts new-onset type 2 diabetes independently of classical risk factors, metabolic syndrome, and C-reactive protein in the West of Scotland Coronary Prevention Study. *Diabetes*. 2004;53:2855-60.
[22] Belluzzi JD, Wang R, Leslie FM. Acetaldehyde enhances acquisition of nicotine self-administration in adolescent rats. *Neuropsychopharmacology*. 2005;30:705-12.
[23] Seeman JI, Dixon M, Haussmann HJ. Acetaldehyde in mainstream tobacco smoke: Formation and occurrence in smoke and bioavailability in the smoker. *Chemical Research in Toxicology*. 2002;15(11):1331-50.
[24] Ernstgård L, Iregren A, Sjögren B, Johanson G. Acute effects of exposure to vapours of acetic acid in humans. *Toxicology Letters.* 2006;165(1):22-30.
[25] Bridges J, De Jong W, Hajslava J, Stahl D. Scientific Committee on Emerging and Newly-Identified Health Risk. *European Communication.* 2008;91.
[26] Linck VM, da Silva AL, Figueiró M, Piato ÂL, Herrmann AP, Birck FD, Caramão EB, Nunes DS, Moreno PRH, Elisabetsky E. Inhaled linalool-induced sedation in mice. *Phytomedicine*. 2009;16(4):303-7.
[27] Hosseinzadeh H, Imenshahidi M, Hosseini M, Razavi BM. Effect of linalool on morphine tolerance and dependence in mice. *Phytotherapy Research.* 2012;26(9):1399-404.
[28] Souto-Maior FN, De Carvalho FLD, De Morais LCSL, Netto SM, De Sousa DP, De Almeida RN. Anxiolytic-like effects of inhaled linalool oxide in experimental mouse anxiety models. *Pharmacology and Biochemistry Behavior*. 2011;100:259-63.
[29] Baumes R, Wirth J, Bureau S, Gunata Y, Razungles A. Biogeneration of C_{13}-norisoprenoid compounds: Experiments supportive for an apo-carotenoid pathway in grapevines. *Analytica Chimica Acta*. 2002;458(1):3-14.
[30] Demole E, Berthet D. Identification de la damascénone et de la β-damascone dans le tabac *Burley*. *Helvetica Chimica Acta*. 1971;54(2):681-2.
[31] Burdock GA. Fenaroli's Handbook of Flavor Ingredients, Fourth Edition, in: Fenaroli's Handbook of Flavor Ingredients, 4th ed. 2001;p. 147.
[32] Scientific Committee on Emerging and Newly Identified Health Risks (SCENIHR). Addictiveness and attractiveness of tobacco additives, *European Commission*. 2011.
[33] Schubert J, Luch A, Schulz TG. Waterpipe smoking: Analysis of the aroma profile of flavored waterpipe tobaccos. *Talanta*. 2013;115:665-74.
[34] Mahmoud BK, Hamed ANE, Samy MN, Abdelmohsen UR, Attia EZ, Fawzy MA, Refaey RH, Salem MA, Pimentel-Elardo SM, Nodwell JR, Desoukey SY, Kamel MS. Metabolomic profiling and biological investigation of *Tabebuia aurea* (Silva Manso) leaves, family Bignoniaceae. *Natural Product Research* (Formerly *Natural Product Letters*). 2019;1-6. https://doi.org/10.1080/14786419.2019.1698571.
[35] Goshman LM. Clinical Toxicology of Commercial Products, 5th ed. *Journal of Pharmaceutical Science*. 1985;74(10):1139.
[36] Rankin GO, Yang DJ, Teets VJ, Lo HH, Brown PI. 3,5-Dichloroaniline-induced nephrotoxicity in the Sprague-Dawley rat. *Toxicology Letters*. 1986;30: 173-9.
[37] Lo HH, Brown PI, Rankin GO. Acute nephrotoxicity induced by isomeric dichloroanilines in Fischer 344 rats. *Toxicology*. 1990;63:215-31.
[38] Divi RL, Doerge DR. Mechanism-Based Inactivation of Lactoperoxidase and Thyroid Peroxidase by Resorcinol Derivatives. *Biochemistry*. 1994;33:9668-74.
[39] Duran B, Gursoy S, Cetin M, Demirkoprulu N, Demirel Y, Gurelik B. The oral toxicity of resorcinol during pregnancy: A case report. *Journal of Toxicology: Clinical Toxicology*. 2004;42(5):663-6.
[40] Yamasaki H, Huberman E, Sachs L. Metabolism of the carcinogenic hydrocarbon benzo(a)pyrene in human fibroblast and epithelial cells. II. Differences in metabolism to water-soluble products and aryl hydrocarbon hydroxylase activity. *International Journal of Cancer*. 1977;19(3):378-82.
[41] Shraideh ZA, Najjar HN. Histological changes in tissues of trachea and lung alveoli of albino rats exposed to the smoke of two types of narghile tobacco products. *Jordan Journal of Biological Sciences*. 2011;4(4):219-24.
[42] Koubaa A, Trabelsi H, Masmoudi L, Triki M, Sahnoun Z, Zeghal KM, Hakim A. Water pipe Tobacco Smoking and Cigarette Smoking: Comparative Analysis of the Smoking Effects on Antioxidant Status, Lipid Profile and Cardiopulmonary Quality in Sedentary Smokers Tunisian. *Intenational Journal of Pharmaceutical Science Invention*. 2013;2(4):51-7